polymer

Polymer 41 (2000) 6635–6645

Rubber toughening of syndiotactic polystyrene and poly/(styrene/diphenylethylene)

F. Ramsteiner*, G.E. McKee, W. Heckmann, S. Oepen, M. Geprägs

BASF Aktiengesellschaft, Kunststofflaboratorium, D-67056 Ludwigshafen, Germany

Received 28 July 1999; received in revised form 26 October 1999; accepted 24 November 1999

Abstract

The high temperature application of styrenic polymers was extended beyond the glass transition temperature of amorphous PS by the two following modifications:

1. Increasing the syndiotactic portion, producing crystallites, which act as physical cross-links in the temperature region between the glass transition and the melting point.
2. Copolymerisation with DPE leading to an increase in the glass transition temperature with increasing DPE-content.

In both materials crazing prevails. Toughness has been successfully improved by rubber modification, by which the initiation and stabilisation of the deformation processes—mostly voiding and crazing—are enhanced. Due to the higher stiffness of the molecules in S/DPE and the mutual interaction between the propagating crazes and the crystalline lamellae in sPS, the rubber toughening in these two types of products is likely to be reduced compared to an amorphous PS. © 2000 Elsevier Science Ltd. All rights reserved.

Keywords: Syndiotactic polystyrene; Poly/(styrene/diphenylethylene); Copolymerisation

1. Introduction

Amorphous polystyrene (aPS) is a very versatile polymer. Its application at high temperature is, however, limited by softening at the glass transition temperature near 100°C. To overcome this limit two modifications of the polystyrene have been performed.

First, syndiotactic polystyrene (sPS) has been produced, whose crystalline phase acts as physical cross-links up to its melting point of nearly 275°C. These crystallites stop material flow above the material's glass transition temperature.

Second, styrene was copolymerised with the stiff diphenylethylene monomer (S/DPE, Fig. 1) leading to an increase in the glass transition temperature.

At room temperature, both modified polymers are as brittle as the amorphous polystyrene. The high stiffness of these polystyrene materials is caused by the restricted mobility of the molecules, accompanied, however, by severely hindered energy dissipative plastic deformation in the bulk. A well-known procedure to stabilise the deformation processes inherent to the material is based on its modification by small rubber particles. In the stress field of the rubber particles numerous sites for the initiation of the deformation processes are formed avoiding premature local overloading of a single deformation zone and fracture.

To explain the extended application of the rubber modified polystyrene-polymers to higher temperatures the following topics are considered: the increased stiffness of the polymers above the glass transition temperature, the compatibility of the rubber particles with the matrix, the deformation modes, and the toughening mechanisms at room temperature.

2. Materials and specimen preparation

sPS has been synthesised by using the method of Ishihara et al. [1]. The sPS content from ^{13}C NMR spectroscopy at

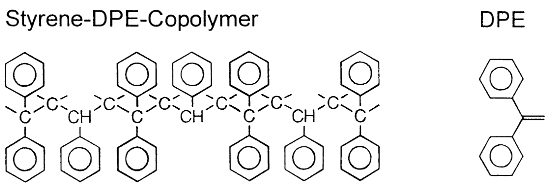

Fig. 1. Structure of S/DPE.

---

* Corresponding author. Tel.: + 49-621-602-2185; fax: + 49-621-609-2281.

E-mail address: falko.ramsteiner@basf-ag.de (F. Ramsteiner).

PII: S0032-3861(99)00863-0

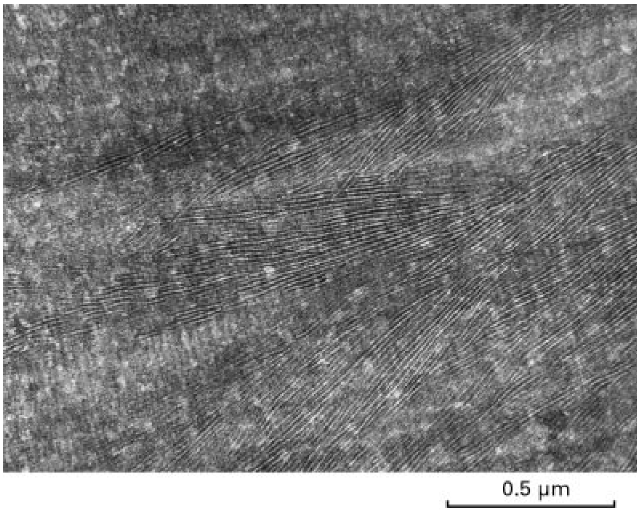

Fig. 2. Crystalline lamellae in sPS.

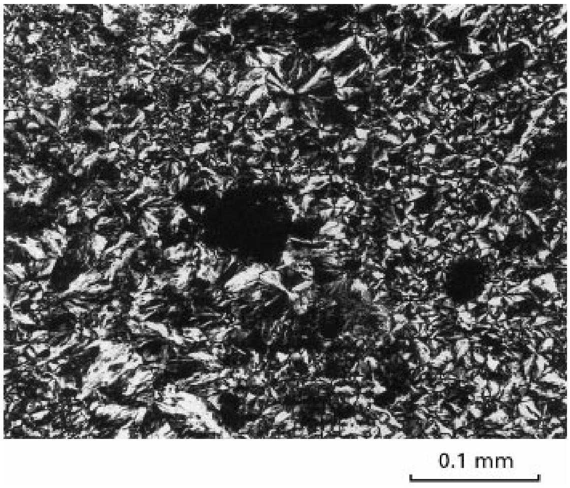

Fig. 3. Spherulites in sPS in polarized light.

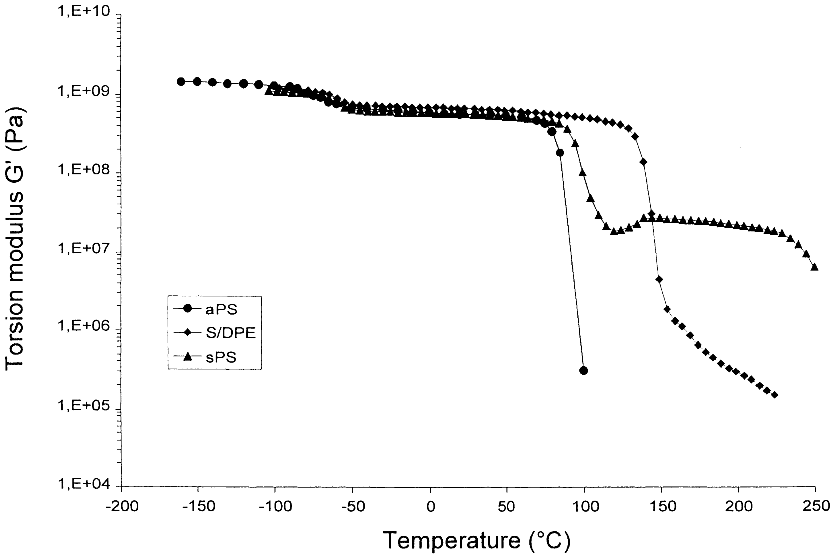

Fig. 4. Dynamic torsion modulus of rubber modified aPS, S/DPE, and sPS as a function of temperature.

130°C in $C_2D_2Cl_4$ was $> 98,5\%$ racemic triads. $M_w = 246\,0000$, $D = 2,5$ from GPC at 130°C in 1,2,4 Trichlorobenzene versus PS standards. Melting point $T_m = 271°C$ from DSC with 20 K/min heating rate.

Styrene/1,1-diphenylethylene copolymers were synthesised by continuous anionic polymerisation in cyclohexane as a solvent and sec-butyllithium as an initiator [2–6].

Impact modified resins were produced by mixing sPS or the S/DPE copolymers with Kraton G1651[1] in a twin screw extruder. Afterwards, the compounds were injection moulded to form dumb bell test pieces.

For transmission electron microscopy (TEM) cryo ultrathin sections were prepared and stained with RuO_4 in the gas phase. For the diffusion measurements the surface of one of the polymer samples was marked by 10 nm colloidal gold particles (Polysciences, Inc.).

3. Measurements

3.1. Stiffness

sPS is a semi-crystalline material, where the crystalline lamellae (Fig. 2) are arranged in spherulites (Fig. 3), which is typical for semi-crystalline polymers. The crystallinity depends on the temperature profile during the cooling

---

[1] Hydrogenated styrene–butadiene–styrene block coploymer (18:64:18 wt%) with a molecular weight of 180 000 g/mol.

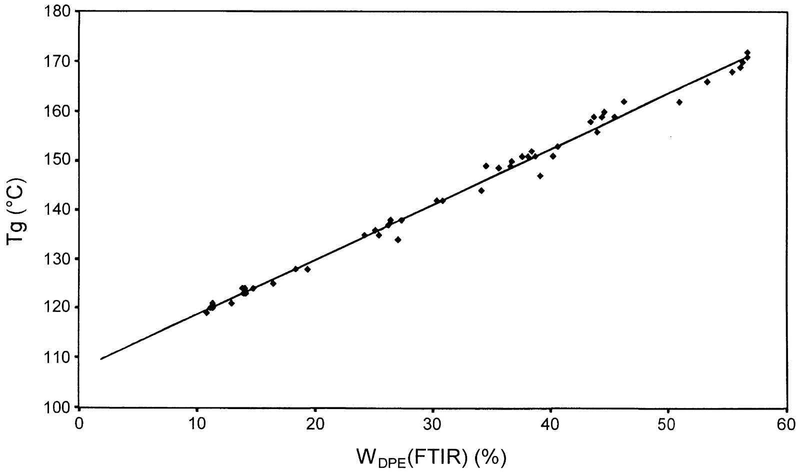

Fig. 5. Increase of the glass temperature (DSC) of S/DPE as a function of the weight content of DPE.

phase of the polymer from the melt into the solid state. S/DPE is, on the contrary, an amorphous polymer.

Fig. 4 shows the torsion dynamic modulus (ISO 6721-7) of the rubber modified atactic and syndiotactic polystyrenes as well as of the poly(styrene diphenylethylene) copolymer. In all three materials the glass transition temperature of the rubbery phase consisting of the hydrogenated polybutadiene is localised near −70°C, therefore the impact modification is expected to work above this temperature, at least in principle. The glass transition temperature of the matrix polystyrene in sPS and aPS is roughly the same and near 100°C. However, the stiffness of sPS is higher than in aPS in the region between the glass transition temperature and the melting point near 275°C due to the cross-linking effects of the crystallites and their reinforcing effects as a filler. This is especially pronounced if the cooling rate from the melt into the solid state has been slow and cold crystallisation between 120 and 140°C (Fig. 4) is not observed during subsequent heating above the glass transition temperature. In S/DPE, high stiffness is present up to the glass transition temperature which increases, compared to aPS by about 1°C/1%DPE (Fig. 5).

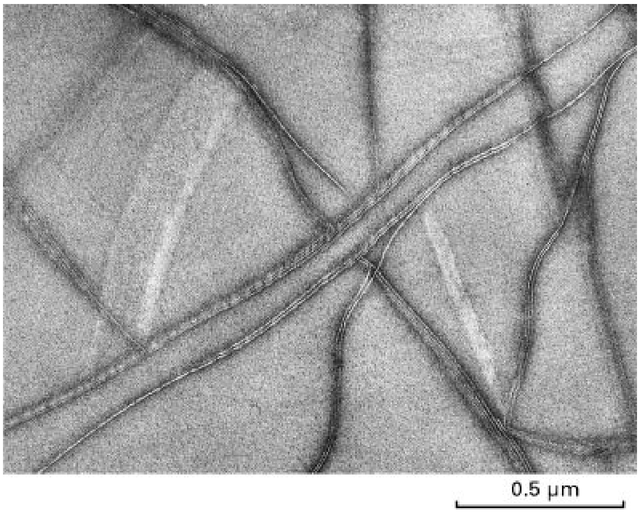

Fig. 6. TEM image of crystalline lamellae in the mixture of 5% sPS in aPS.

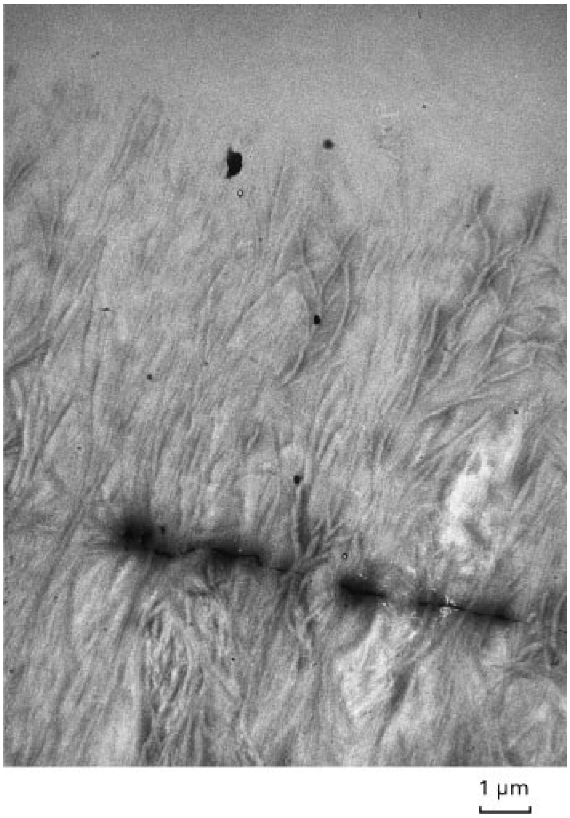

Fig. 7. TEM image of the interdiffusion zone at the interface of aPS (upper part) and sPS (lower part) after annealing at 290°C for 30 min. Before welding the original interface was marked by colloidal gold particles.

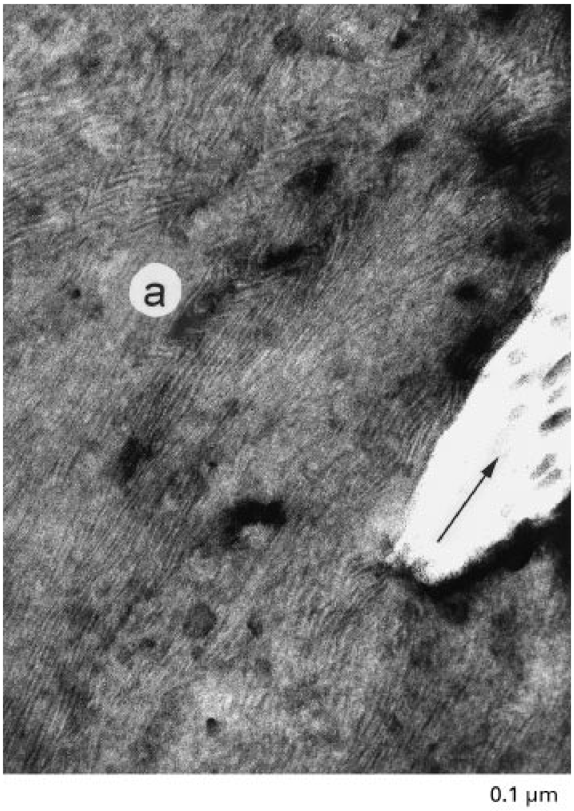

Fig. 8. TEM image of sheared crystalline lamellae in rubber modified sPS after deformation at 110°C in tension. Herring bone pattern is visible near a. The arrow in the elongated rubber particle indicates the tensile direction.

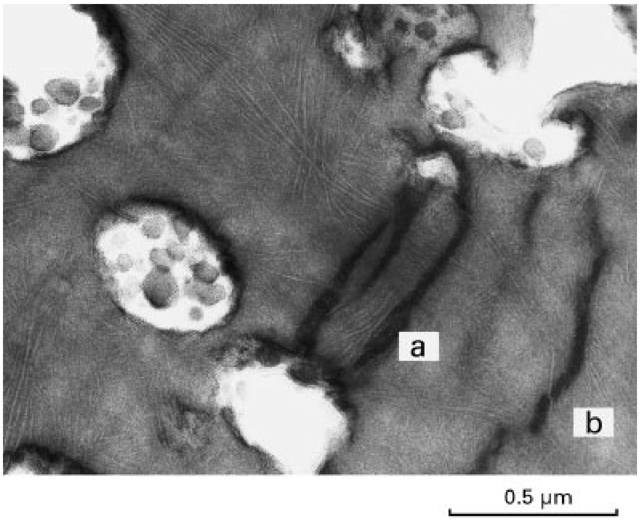

Fig. 10. Interaction between crazes and cristalline lamellae in sPS: (a) craze propagate between lamellae; (b) crystalline lamellae are kinked by crazes.

3.2. Compatibility

In the rubber modification of sPS and S/DPE copolymers the rubber phase is compatibilised with the different polystyrene matrices via the atactic polystyrene blocks in the Kraton. This compatibilisation increases both the dispersion of the particles in the matrix and the adhesion between the rubbery particles and the matrix.

sPS is compatible with aPS in the melt [7]. In the solid state the aPS is included into the amorphous region of sPS. This is shown for a mixture of 5% sPS in aPS (Fig. 6) where the crystalline lamellae are well dispersed in the whole aPS-matrix. No agglomeration of sPS to spherical regions is observed. To demonstrate the interdiffusion of both polystyrene-types two pieces of each material were brought in contact after having marked the interface with gold. After annealing at 290°C for 30 min, sPS has grown into the amorphous phase of aPS to a depth of about 8 μm (Fig. 7).

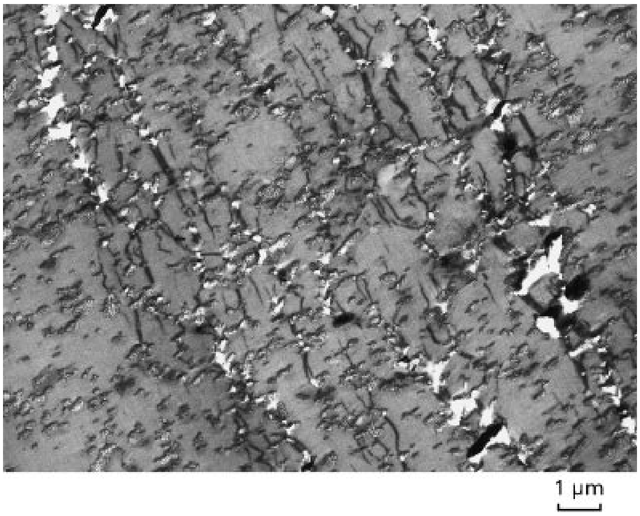

Fig. 9. TEM image of crazes in rubber modified sPS after deformation.

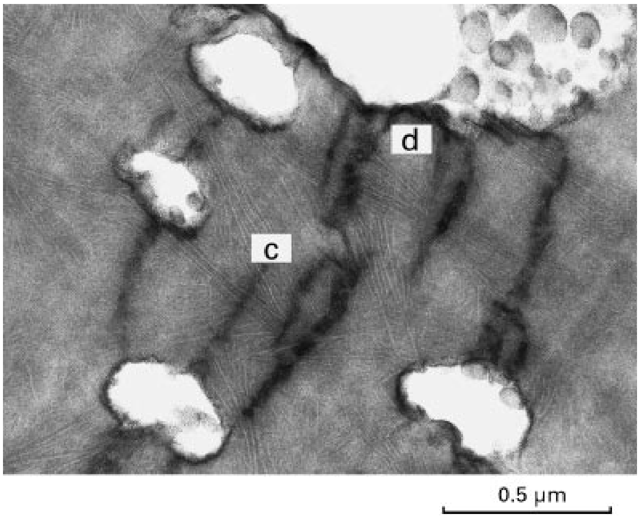

Fig. 11. Interaction between crazes and crystalline lamellae in sPS: (c) crazes are deflected by stacks of inclined crystalline lamellae; (d) crazes are hindered in opening by perpendicular crystalline lamellae.

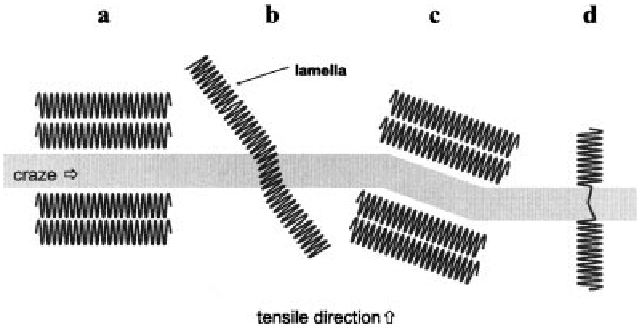

Fig. 12. Scheme of the interaction between crazes and different oriented crystalline lamellae.

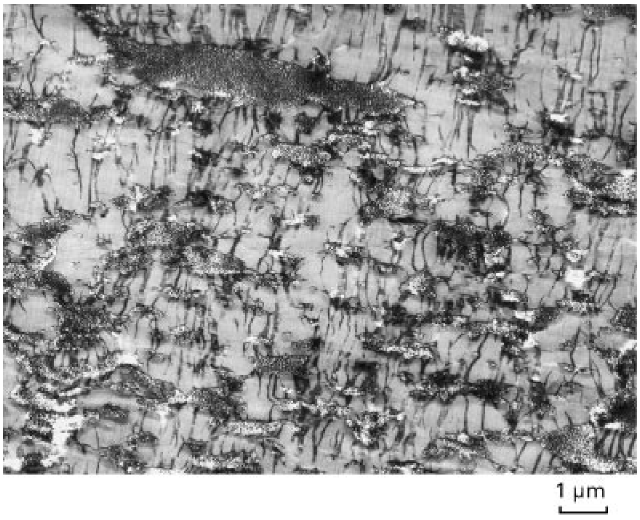

Fig. 13. TEM image of crazes in rubber modified S/DPE after deformation.

S/DPE is completely compatible with PS only for DPE-concentrations below 15% as can be shown by DSC [8]. Therefore additional compatibilisers might be helpful for a DPE-rich matrix.

3.3. Deformation modes

Above the glass transition temperature shear deformation prevails in the sPS matrix since the molecules in the amorphous region are mobile. The herring bone pattern of the crystalline lamellae originally running perpendicular to the tensile direction is observed (Fig. 8) under the transmission electron microscope. This pattern can be explained by assuming shearing along the molecules within the lamellae as is known for the semi-crystalline polymers [9,10]. The material is tough at higher temperatures.

For practical reasons the deformation at room temperature and lower is more important than that above the glass transition temperature for both materials. When rubber modified sPS is deformed below the glass transition temperature crazes are formed as shown in the TEM image in Fig. 9. At higher magnification (Figs. 10 and 11) the interaction between the crystalline lamellae and the propagating crazes can be observed. In the region where lamellae are perpendicular to the tensile direction crazes propagate between them within the amorphous region (Fig. 10a). If the crazes cross lamellae oblique to the propagation direction the lamellae become very often kinked (Fig. 10b) or deflected (Fig. 11c). In regions where lamellae are oriented in the tensile direction the fibrillation within the crazes seem to be restricted (Fig. 11d). Schematically these

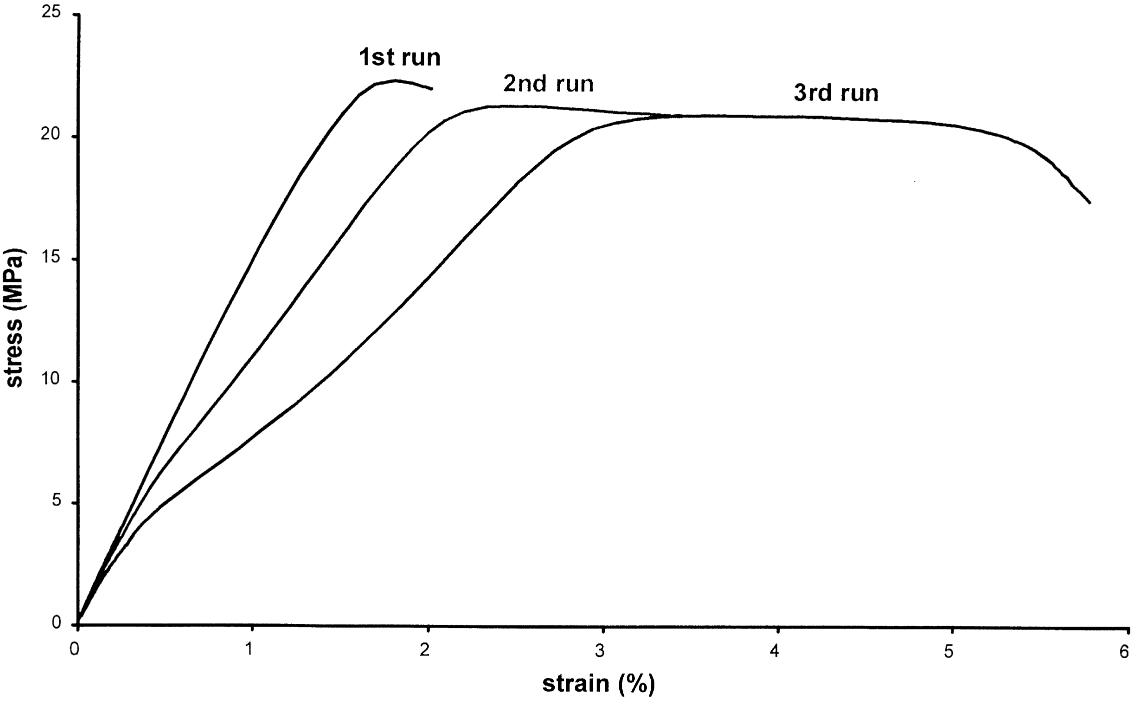

Fig. 14. Loading/unloading/loading cycles of sPS (specimen annealed 30 min at 180°C).

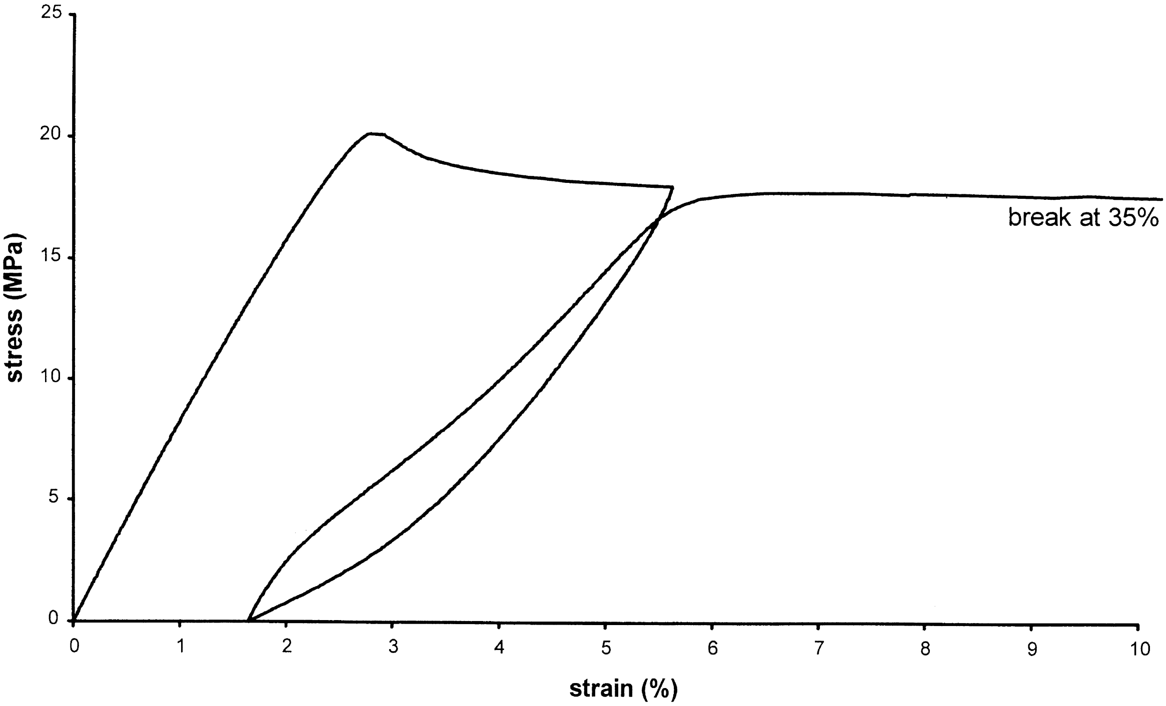

Fig. 15. Loading/unloading cycle of S/DPE.

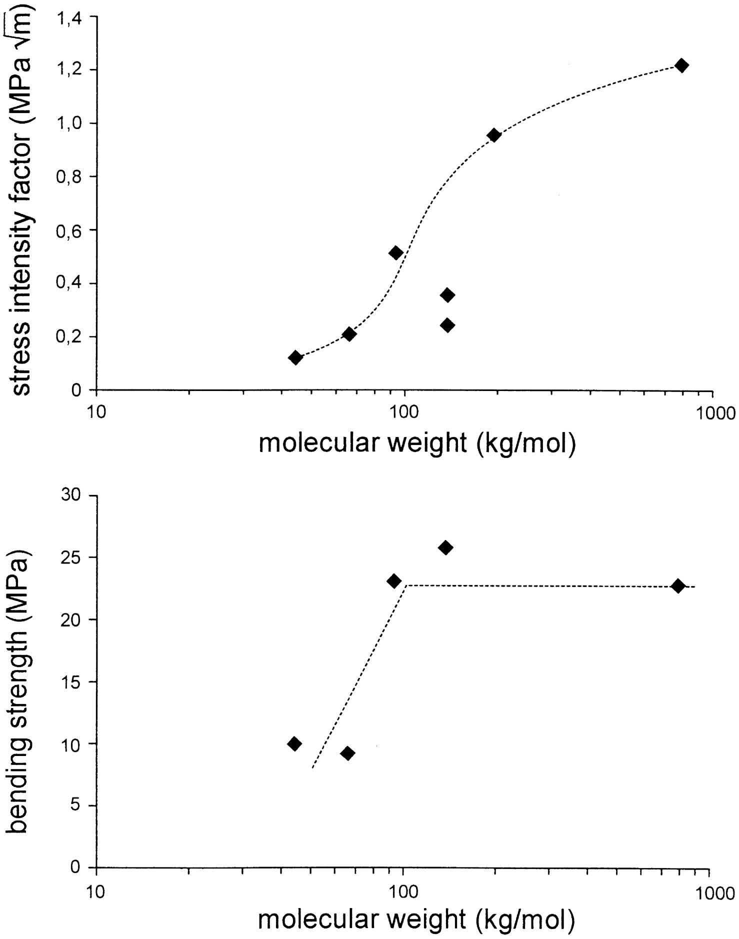

Fig. 16. Stress intensity factor (upper picture) and bending strength (lower picture) of sPS as a function of molecular weight.

Table 1
Notched impact strength a_k (kJ/m^2) of styrene-polymers with 35% Kraton for various processing conditions. ((inj.m.) injection moulded at different mould temperatures, (anneal.) annealing)

Material	Rubber modified sPS			sPS			Rubber modified S/DPE			
							(15%DPE)		(30%DPE)	
Processing	inj.m.	inj.m.	Anneal.	inj.m.	inj.m.	Anneal.	inj.m.	Anneal.	inj.m.	Anneal.
Melt temperature	290	290	30 min/180°C	290	290	30 min/180°C	250	30 min/180°C	250	30 min/180°C
Mould temperature (°C)	80	120		60	140					
a_k (kJ/m^2)	6.0	3.7	2.7	0.6	0.6	0.5	23	12	15	6

four possibilities are sketched in Fig. 12 in an idealised manner.

The TEM image of S/DPE cut parallel to the tensile direction is shown in Fig. 13. Crazes running between the rubber particles combined with voiding in the rubbery phase are the main energy dissipation processes.

The volume change of the rubber modified sPS in a fluid dilatometer [11] yields about 80% voiding in the injection moulded specimens and 87% in the annealed specimen. This total voiding is caused by both the volume change by crazing and voiding in the rubbery phase. In rubber modified S/DPE total voiding is responsible for about 60% of the deformation.

Characteristic of crazing in HIPS and ABS [12,13] is the entropy deformation of the fibrils in the crazes in hysterese experiments, where the specimen is first deformed, unloaded and reloaded again. The force–deflection curve in the second run is S-shaped when crazes have been formed during the first run. Fig. 14 shows the loading/unloading/reloading curves of the specimen of the rubber modified sPS in the annealed state. If the deformation is high enough to produce craze deformation during the 1st run, the S-shaped curve for craze deformation as mentioned before is evident. It must be concluded that crazing plays an important role in the deformation of rubber modified sPS, in complete accordance with the findings from the TEM images.

Loading/unloading/reloading experiments with S/DPE (Fig. 15) confirm crazing as expected from the TEM results.

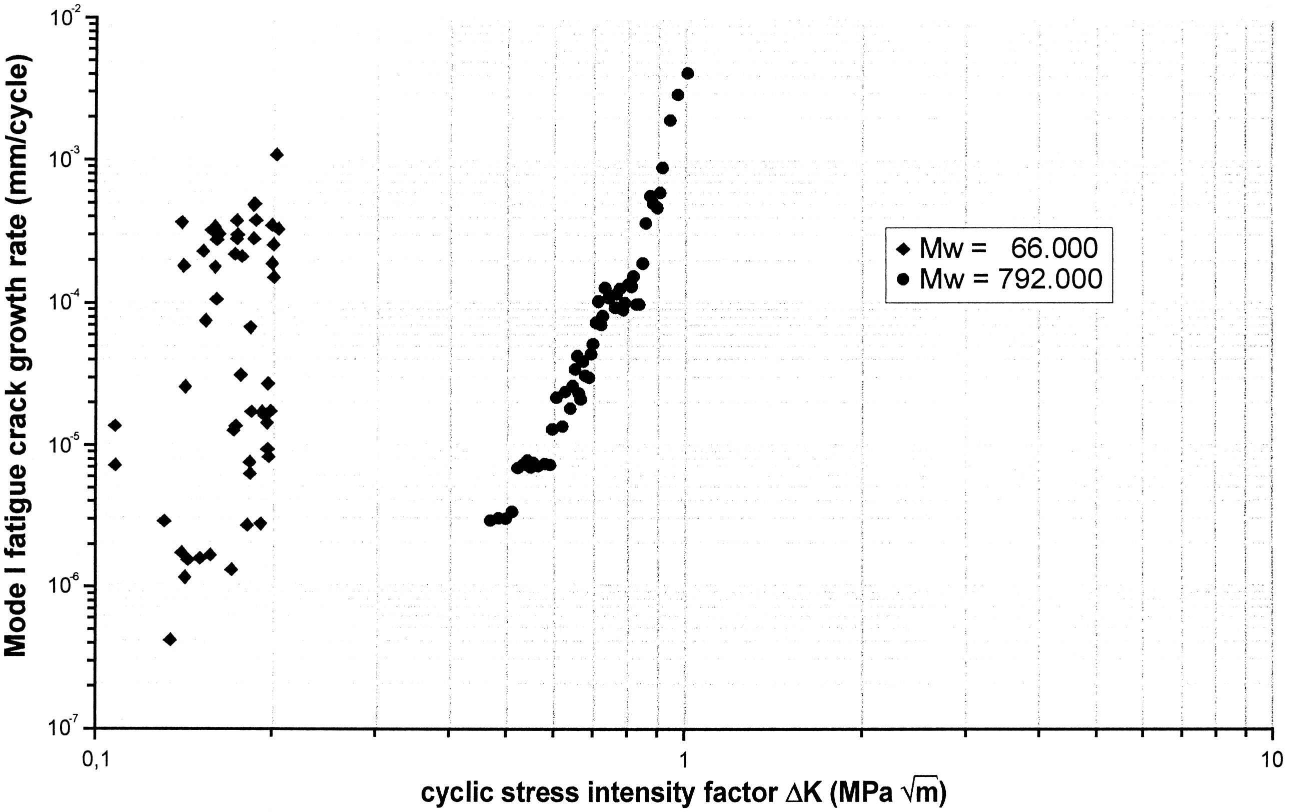

Fig. 17. Crack growth rate as a function of stress intensity amplitude in fatigue test at 10 c/s.

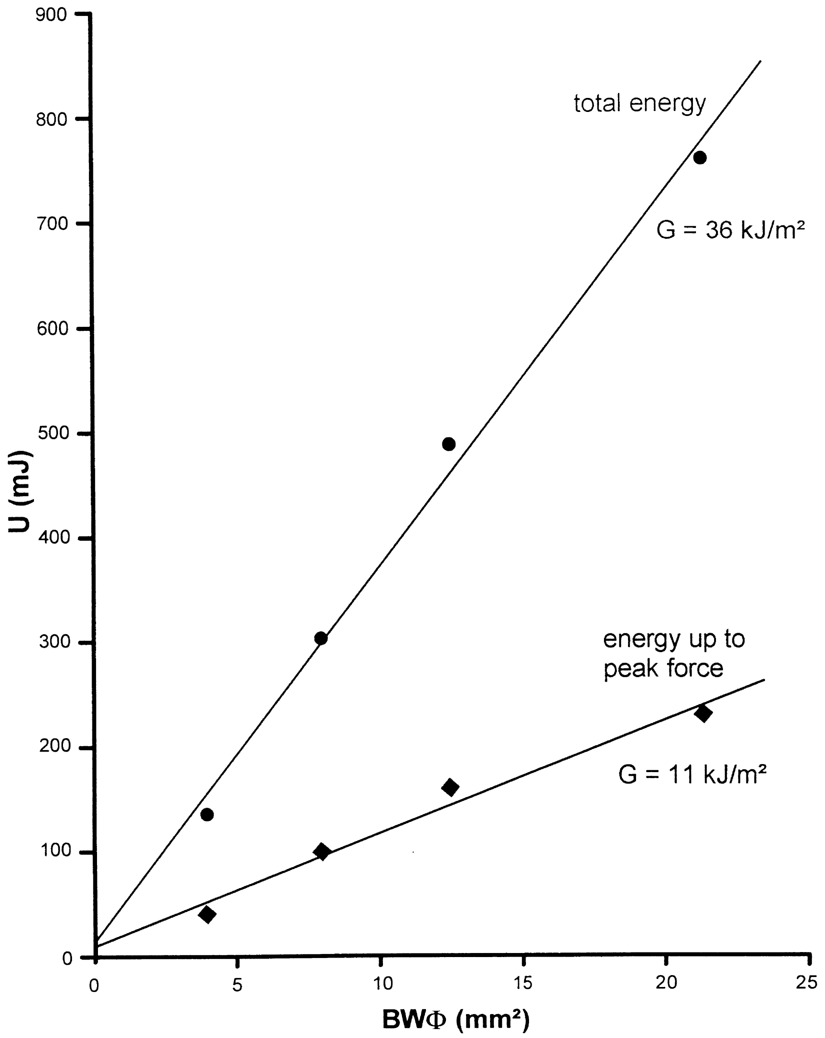

Fig. 18. Apparent energy release rate determination of S/DPE (15%) in impact up to the peak stress and total fracture.

3.4. Toughness in impact

The notched impact strengths at 23°C are summarised in Table 1 for the materials described in this paper.

By rubber modification notched impact strength of sPS was increased from 0.6 kJ/m^2 for the pure sPS under the most favourable conditions by an order of magnitude up to 6 kJ/m^2 (Table 1). When it is injection moulded using a high mould temperature (120°C) crystallinity in the specimen is likely to be higher than at the lower mould temperature (80°C). DSC measurements [8] yield 18% crystallinity for injection into a mould at 80°C, 33% for the 120°C mould and 60% for the annealed material. This increased crystallinity reduces the toughness due to the smaller amorphous region, where the fibrillation within crazes preferentially occurs. The force deflection diagrams show the brittleness to be caused by reduced strain at fracture and not by lower failure forces. Additionally the increased interaction between crazes and crystalline lamellae as shown in Figs. 10 and 11 may also decrease toughness. A reduced orientation of the molecules can, on one hand, increase toughness by facilitating energy dissipating crazing and can, on the other hand, reduce toughness by reducing the strength of the polymer. The final result of these competing effects depends on the details. On annealing the specimens the notched impact strength is reduced. In the present case, notched impact strength appears to be increased by higher orientation and reduced crystallinity. Pure sPS is brittle and its toughness nearly independent of the processing parameters.

A prerequisite for toughness is that the molecular weight of the sPS is high enough to form an entangled network. In Fig. 16 the apparent stress intensity factor K_Q according to Ref. [14] and the bending strength are plotted as a function of the molecular weight. For the formation of tie molecules (entanglements) and thus for high strength the molecular weight of the sPS should be higher than 100 000 g/mol.

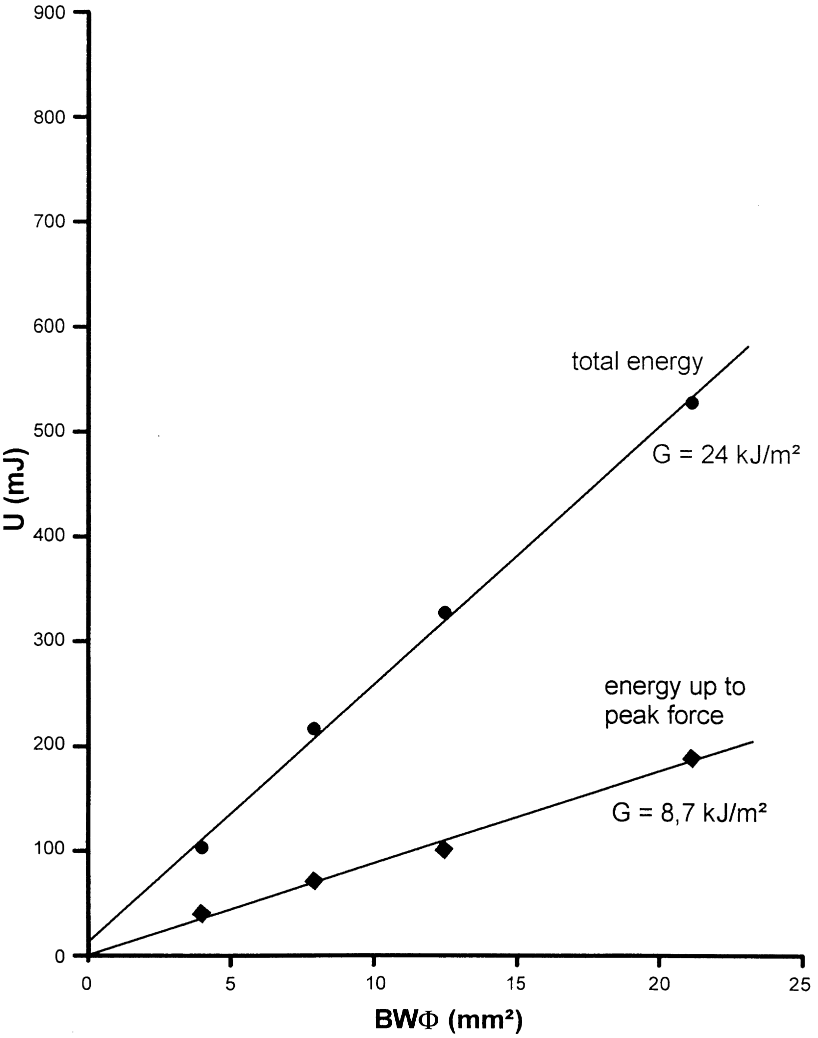

Fig. 19. Apparent energy release rate determination of S/DPE (30%) in impact up to the peak stress and total fracture.

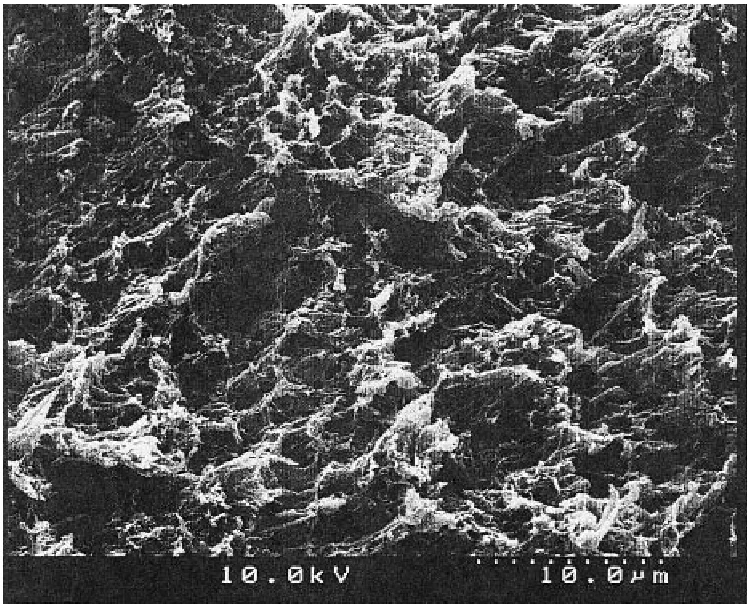

Fig. 20. REM image of the fracture surface of sPS.

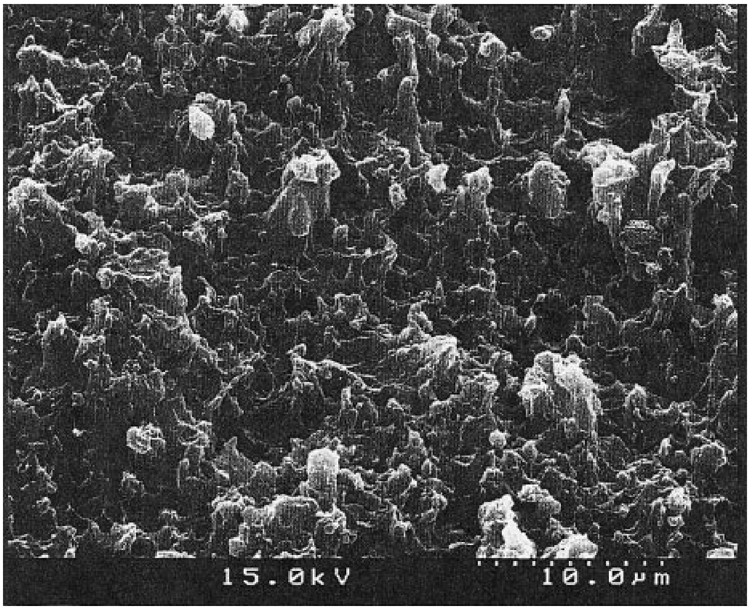

Fig. 21. REM image of the fracture surface of S/DPE (15%).

This limit is in accordance with the results from neutron scattering experiments [15]. Crack propagation in sPS measured in fatigue tests at 10 c/s is as expected much faster (Fig. 17) in the lower molecular weight sPS (66 000) than in the higher (792 000) one.

In the amorphous S/DPE copolymer the toughening effect of the rubber is more pronounced with 15% than with 30% DPE comonomer (Table 1). The reason is probably to be found in the higher stiffness of the S/DPE (30) and its reduced compatibility with the polystyrene of the Kraton block copolymer. Reduced orientation of the molecules by annealing of the specimen reduced toughness further.

In Fig. 18 the fracture mechanical evaluation [16,17] of the energy release rate according to the standard procedure is shown for S/DPE (15%) and in Fig. 19 for the S/DPE (30%). Both materials do not exhibit a brittle fracture thus linear fracture mechanics are not applicable. But we learn, however, from these plots that the apparent energy release rate up to the peak stress where failure starts is higher in the material with the lower DPE content (10.8 vs. 8.7 kJ/m^2).

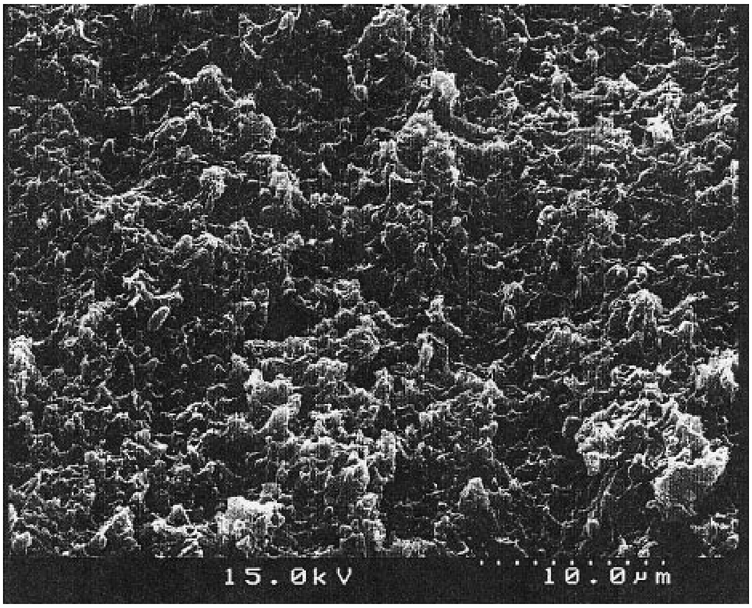

Fig. 22. REM image of the fracture surface of S/DPE (30%).

This difference holds also for the total energy dissipation which also includes the plastic deformation processes (35.7 vs. 24.4 kJ/m^2). These results correlate with the notched impact strengths in Table 1 and seem to reflect the restricted deformation of the material with increasing content of the stiff DPE portion.

Figs. 20–22 show the fracture surfaces of the rubber modified sPS, S/DPE (15%), and S/DPE (30%) using scanning electron microscopy. In all the three cases the fracture surface shows enhanced fibrillation due to deformation. The adhesion between the matrix and the rubber particles seems to be strong enough for their deformation in all the three materials. Isolated rubber particles, however, cannot be observed.

4. Discussion

Amorphous PS finds widespread use due to its high stiffness. This advantageous property is enhanced in polymers by low mobility of the polymer molecules in the bulk product. The disadvantage, however, is increased brittleness. Therefore if the application also requires toughness, PS is modified with rubber particles as, for example, in HIPS. A further disadvantage is that this material softens near the glass transition temperature of the polystyrene of 100°C, barring its applications at higher temperatures. To increase its maximal usable temperature the PS matrix has been modified in the following two ways. Firstly by increasing the syndiotacticity which allows crystals to be formed, which act as physical cross-links up to their melting point near 275°C and secondly by copolymerisation with DPE, which increases the glass transition temperature at a rate of 1°C/1% DPE. Increased toughness, characterised by the notched impact strength and the energy release rate, was attained in both materials in an analogous way to aPS by rubber modification. In both modified styrene-materials crazing combined with voiding in the rubbery phase are the dominant deformation processes, which must be enhanced to toughen the material. The mechanical relevant influence of voiding and crazing on toughness was proved by SEM images of the fracture surfaces, TEM, hysteresis and dilatational measurements. Propagating crazes and crystalline lamellae were shown to interact in different ways depending on their orientation to one another. A prerequisite for rubber toughening is, in addition to a sufficiently high molecular weight of the matrix, the adhesion of the rubber particles to the matrix. The compatibility of both was proved by an interdiffusion test and from SEM of fracture surfaces where no isolated rubber particle could be seen. Beyond the screening tests described in this paper, there is plenty of room to optimise the toughness of PS-based materials for application at higher temperatures.

Acknowledgements

The authors acknowledge the experimental support of this work by S. Forster, T. Armbrust and R. Walter.

References

[1] Ishihara N, Seimiya T, Kuramoto M, Uoi M. Macromolecules 1986;19:2464.
[2] Priddy DB. Adv Polym Sci 1994;111:67.
[3] Yuki H, Kosai K, Murahashi S, Hotta J. J Polym Sci, Part C: Polym Lett 1964;2:1121.
[4] Ureta E, Smid J, Szwarc M. J Polym Sci: Part A-1 1966;4:2219.
[5] Yuki H, Hotta J, Okamoto Y, Murahashi S. Bull Chem Soc Jpn 1967;40:2659.
[6] Yuki H. Prog Polym Sci 1972;3:141.
[7] Bonnet M, Buhk M, Trögner G, Rogausch K-D, Petermann J. Acta Polym 1996;49:174.
[8] Hennig, I. Private communication.
[9] Kanig G. Progr Colloid Sci 1975;57:176.
[10] Lin L, Argon AS. J Mater Sci 1994;29:294.
[11] Ramsteiner F. Polym Testing 1996;15:401.
[12] Kambour RP, Kopp RW. J Polym Sci A 1969;2:183.
[13] Ramsteiner F, McKee GE, Fischer W, Fischer M. Acta Polym 1997;48:553.
[14] ISO DIS 13586.
[15] Moyses S, Spells SJ. Polymer 1999;40:3269.
[16] ISO CD 17281.
[17] Ramsteiner F. In: Grellmann, Seidler, editors. Deformation und Bruchverhalten von Kunststoffen, Berlin: Springer, 1998.